

FSU-HEP-950311

THE SEARCH FOR SUPERSYMMETRY

HOWARD BAER

*Dep't of Physics, Florida State University
Tallahassee, FL 32306, USA
E-mail: baer@hep.fsu.edu*

ABSTRACT

The minimal supergravity model (SUGRA), with gauge coupling unification and radiative electroweak symmetry breaking, is a well-motivated paradigm for physics Beyond the Standard Model. In this talk, I review the capabilities of various present and future collider experiments to make definitive tests of the SUGRA model, including LEP and LEP II, the Tevatron and its upgrades, and finally the CERN LHC project.

1. Introduction

When Dirac first incorporated Lorentz symmetry into quantum mechanics, he found that every known particle had to have a “partner” particle, the anti-particle. When supersymmetry, which is a natural generalization of the Lorentz group, is incorporated into the framework of quantum field theory, once again, all known particles are found to have partners: the so-called sparticles. Although supersymmetry was “discovered” in a mathematical sense in the late 1960’s and 1970’s, a supersymmetric version of the Standard Model (SM) did not emerge until the early 1980’s¹. The resulting theory, often called the Minimal Supersymmetric Standard Model (MSSM)², is looked upon as a likely low energy effective theory of some more fundamental superstring or supergravity GUT model. Recent precision measurements of gauge couplings at LEP, when extrapolated to ultra-high energy scales via renormalization group equations, achieve unification at a scale $M_X \sim 2 \times 10^{16}$ GeV in the MSSM, but not in the SM³. This fact has led to intense scrutinization of supersymmetric models with unification.

The minimal supergravity model is “minimal” in the sense that only the minimal number of new particles and interactions are introduced to be consistent with phenomenology. In particular, this implies that R -parity is conserved. It is “super”-symmetric, in that the Lagrangian possesses supersymmetry, and hence predicts super-partners. The supersymmetry is broken by including soft-supersymmetry breaking terms, which parametrize our ignorance of the exact mechanism of supersymmetry breaking. “Gravity” enters by assuming a simple structure for the soft-supersymmetry breaking terms at or beyond the unification scale. For instance, if supersymmetry is broken in a hidden sector of the model at very high energy scales, the breaking can be communicated to the observable sector by gravitational interactions, which

are universal in strength. This leads to a common mass m_0 for all scalar soft-breaking terms, a common gaugino mass $m_{1/2}$ for the three soft-breaking gaugino masses, and common trilinear couplings A_0 and a bilinear term B_0 . Starting from the unification scale, the various couplings and masses are evolved via renormalization group equations, which yield the low energy (weak-scale) running sparticle masses and couplings. A consequence of this mechanism is that electroweak symmetry is broken when one of the Higgs mass squared terms is driven negative. Ultimately, the whole low energy superparticle spectrum can be calculated in terms of the parameter set

$$m_0, m_{1/2}, A_0, \tan \beta, \quad (1)$$

along with the sign of the superpotential Higgs mass μ and the top mass m_t .

2. Connection to experiment

The above framework is simple, well-motivated, compelling, consistent with data, and testable, since the soft supersymmetry breaking terms are expected to be generally of order the weak scale: $\sim 100 - 1000$ GeV. The key to connecting the SUGRA framework with experiment lies in the event generator program. Recently, the MSSM, and in addition, the more constrained SUGRA framework, has been incorporated into the event generator program ISAJET⁴, so that super-particle production and decay can be simulated for e^+e^- , $p\bar{p}$ or pp colliders.

To simulate sparticle production and decay at a hadron collider, the following steps are taken using ISAJET 7.13:

- input the parameter set $(m_0, m_{1/2}, A_0, \tan \beta, \text{sign}(\mu), m_t)$, (or a less constrained MSSM set),
- all sparticle and Higgs masses and couplings are computed,
- all sparticle, top and Higgs decay modes and branching fractions are calculated,
- all lowest order $2 \rightarrow 2$ sparticle production processes are calculated (if desired, subsets of the reactions can be selected),
- the hard scattering is convoluted with parton distribution functions,
- initial and final state QCD radiation is calculated with the parton shower model,
- particles and sparticles decay through their various cascades,
- quarks and gluons are hadronized, and heavy hadrons are decayed,
- the underlying soft scattering of beam remnants is modelled,

- the resulting event and event history is generated for interface with detector simulations, or for direct analysis.

For e^+e^- collisions, the steps are similar, except that initial state QCD radiation, PDF convolution and beam jet evolution do not enter.

3. Sparticles at LEP and LEP II

The four LEP experiments have placed relatively model independent bounds of the masses of various sparticles and Higgs bosons⁵. To be specific⁶,

$$\begin{aligned}
m_{\tilde{W}_1} &> 45 \text{ GeV}, \\
m_{\tilde{Z}_1} &> 18 \text{ GeV, (GUT relation assumed)}, \\
m_{\tilde{\ell}} &> 45 \text{ GeV, } (\tilde{\ell} = \tilde{e}, \tilde{\mu}, \tilde{\tau}), \\
m_{\tilde{q}} &> 45 \text{ GeV}, \\
m_{\tilde{\nu}} &> 41.8 \text{ GeV, (three degenerate flavors)}, \\
m_{H_\ell} &\gtrsim 60 \text{ GeV}.
\end{aligned}$$

The above sparticle mass limits are mainly limited by the beam energy. Hence, considerable improvement is soon expected from the energy upgrade to LEP II, running at $\sqrt{s} = 150 - 190$ GeV, at integrated luminosity of $300 - 500 \text{ pb}^{-1}$ per year.

Roughly then, LEP II is expected to probe slepton, chargino and squark masses to ~ 90 GeV, as well as the light MSSM Higgs boson to ~ 90 GeV. The m_0 vs. $m_{1/2}$ plane seems to provide a convenient panorama in which to plot results⁷. In Fig. 1, we take $A_0 = 0$, $\tan \beta = 2$ and $m_t = 170$ GeV, and show results for both signs of μ . The gray regions are excluded on theoretical grounds, since in the lower left region, electroweak symmetry breaking does not occur, or cannot attain the proper Z -boson mass. Other parts of the gray regions are excluded because sparticles other than the \tilde{Z}_1 become the LSP. The current experimentally excluded region in Fig. 1a (shown by hatch marks) is due to four separate limits: the LEP limits that $m_{\tilde{W}_1} > 47$ GeV, $m_h \gtrsim 60$ GeV, and $m_{\tilde{\nu}} > 43$ GeV, and also the Tevatron $\cancel{E}_T + \text{jets}$ search. In Fig. 1b, the experimentally excluded region is made up entirely of the LEP chargino mass bound. Future searches at LEP II should probe below the dot-dashed lines, which indicate the 90 GeV contours for $\tilde{\ell}$, \tilde{W}_1 and H_ℓ .

4. Sparticles at the Tevatron and its upgrades

4.1. $\tilde{g}\tilde{g}$, $\tilde{g}\tilde{q}$ and $\tilde{q}\tilde{q}$ signals

Sparticle production at the Fermilab Tevatron collider is dominated by $\tilde{g}\tilde{g}$, $\tilde{g}\tilde{q}$ and $\tilde{q}\tilde{q}$ production as long as $m_{\tilde{g}} < 250 - 350$ GeV. Once these sparticles are produced,

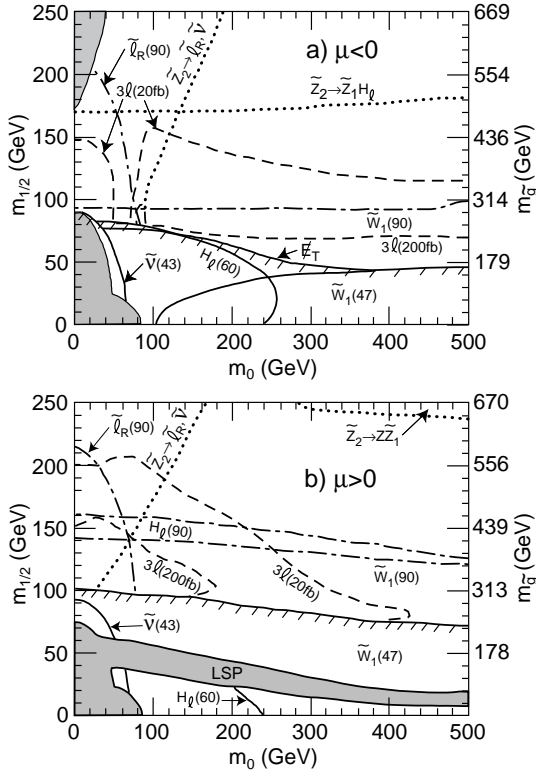


Figure 1: Regions in the m_0 vs. $m_{1/2}$ plane explorable by Tevatron and LEP II experiments.

they decay via cascades through various charginos and neutralinos until the state containing the lightest SUSY particle (LSP) is reached. Thus, the final state consists of multiple leptons, jets and missing energy from undetected LSP's and neutrinos. Searches at the CDF and D0 experiments have mainly focused on the multi-jet + \not{E}_T channel. By seeing no signal above expected background rates, they conclude⁸ (based on $\sim 10 \text{ pb}^{-1}$ of data) that $m_{\tilde{g}} \gtrsim 150 \text{ GeV}$ if $m_{\tilde{g}} \gg m_{\tilde{g}}$, or $m_{\tilde{g}} \gtrsim 210 \text{ GeV}$, if $m_{\tilde{g}} \sim m_{\tilde{g}}$.

The mass reach (in terms of $m_{\tilde{g}}$, for comparison with Fig. 1) of the Tevatron experiments via various multi-isolated-lepton topologies has been calculated in Ref. 9, for 100 and 1000 pb^{-1} of integrated luminosity, for nominal cuts to remove the bulk of background, and are listed in Table 1.

In the main injector (MI) era (integrated luminosity $\sim 1 \text{ fb}^{-1}$), the reach in the $\not{E}_T + \text{jets}$ channel will be background limited. However, in the SS dilepton and 3ℓ channels, a much larger range of masses can be explored. In the 3ℓ channel, for $m_{\tilde{q}} \sim 2m_{\tilde{g}}$, $m_{\tilde{g}} \sim 260 \text{ GeV}$ can be explored, while for $m_{\tilde{q}} \sim m_{\tilde{g}}$, squarks and gluinos

Table 1: Reach in $m_{\tilde{g}}$ via various event topologies for the SUGRA-inspired MSSM, assuming an integrated luminosity of 0.1 fb^{-1} (1 fb^{-1}), at the Tevatron collider. We use $m_t = 150 \text{ GeV}$ for the background.

case	\cancel{E}_T	1ℓ	OS	SS	3ℓ	$\geq 4 \ell$
$m_{\tilde{q}} = m_{\tilde{g}} + 10 \text{ GeV}$	240 (260)	— (—)	225 (290)	230 (320)	290 (425)	190 (260)
$m_{\tilde{q}} = m_{\tilde{g}} - 10 \text{ GeV}$	245 (265)	— (—)	160 (235)	180 (325)	240 (440)	— (—)
$m_{\tilde{q}} = 2m_{\tilde{g}}$	185 (200)	— (—)	— (180)	160 (210)	180 (260)	— (—)

as heavy as 425-440 GeV might be detectable.

4.2. $\tilde{W}_1 \tilde{Z}_2 \rightarrow 3\ell + \cancel{E}_T$ signal

Recently, there has been much interest in the $\tilde{W}_1 \tilde{Z}_2 \rightarrow 3\ell + \cancel{E}_T$ signal, due to its significant signal rate over much of parameter space, and especially the low background rate expected from SM processes¹⁰. Using cuts designed to extract signal from background, detailed simulations of this signal have recently been performed over large regions of SUGRA parameter space, for the Tevatron MI, and also a proposed luminosity upgrade to 25 fb^{-1} per year, dubbed TeV^* . Results are shown, in a wonderful plot by Chen¹⁰, for $\mu < 0$ and $\tan \beta = 2$, in Fig. 2. The black squares indicate the reach of Tevatron MI, while squares with X's and open squares designate the 10σ and 5σ reach of TeV^* . In Fig. 2b, the corresponding \tilde{g} , \tilde{W}_1 and $\tilde{\ell}_R$ mass contours are plotted. Thus, for the low range of m_0 , the MI can probe to $m_{\tilde{g}} \sim 450 \text{ GeV}$, while for large m_0 , MI can probe to $m_{\tilde{g}} \sim 215 - 270 \text{ GeV}$. The reach of TeV^* is considerably greater: $m_{\tilde{g}} \sim 700 \text{ GeV}$ for small m_0 , while $m_{\tilde{g}} \sim 500 \text{ GeV}$ for large m_0 . Unfortunately, this compelling behavior doesn't persist if we switch the sign of μ . For $\mu > 0$, there is an equivalent reach in terms of $m_{\tilde{g}}$ for small m_0 , but for large $m_0 \gtrsim 300 - 400 \text{ GeV}$, interference effects in the $\tilde{Z}_2 \rightarrow \ell \bar{\ell} \tilde{Z}_1$ branching fraction kill the signal, giving no reach at all via clean trileptons¹⁰ for either MI, TeV^* , or even LHC (see Fig. 1b 3ℓ contour).

4.3. Other sparticles

The Tevatron also has the capability to search for light top squarks below about $m_{\tilde{t}_1} \sim 100 \text{ GeV}$ ¹¹. If the decay $\tilde{t} \rightarrow b \tilde{W}_1$ is allowed, it should dominate top squark decays. If so, top squark signatures are the same as top quark signatures, except the decay products are softer. If the $\tilde{t} \rightarrow b \tilde{W}_1$ decay is kinematically closed, then it is expected $\tilde{t}_1 \rightarrow c \tilde{Z}_1$ dominates. In this case, one looks for charm dijet events, plus \cancel{E}_T .

It appears to be difficult to search for sleptons at the Tevatron. The best signature is in the dilepton + \cancel{E}_T channel. Unfortunately, a low signal rate plus large backgrounds from $\tau \bar{\tau}$ and WW production seem to swamp this signal for $m_{\tilde{\ell}} \gtrsim 50$

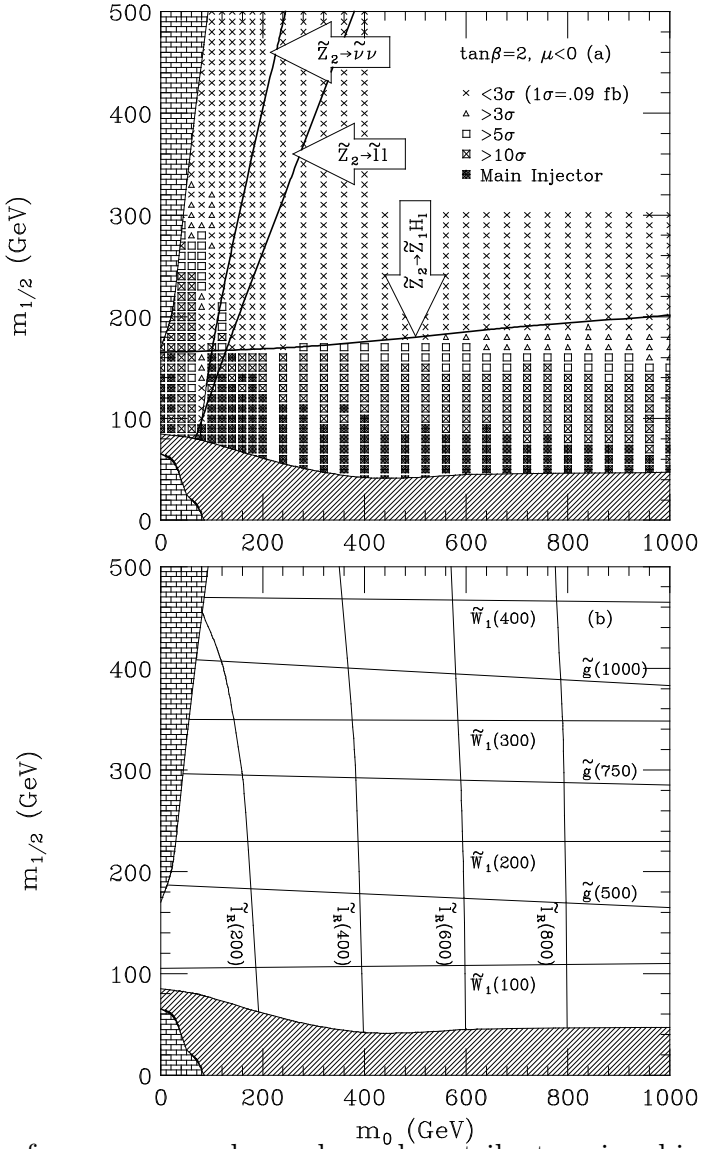


Figure 2: Regions of m_0 vs. $m_{1/2}$ plane where clean trilepton signal is observable over background, for Tevatron MI project (1 fb^{-1}) and TeV* (25 fb^{-1}). We take $A_0 = 0$ and $\mu < 0$.

Table 2: 5σ discovery limits in $m_{\tilde{g}}$ (in TeV) via $\cancel{E}_T + \text{jets}$ events at LHC Atlas detector for various choices of squark and gluino mass ratios, and collider integrated luminosities. Variation of MSSM parameters can cause these limits to vary by ~ 150 GeV.

case	10^3 pb^{-1}	10^4 pb^{-1}	10^5 pb^{-1}
$m_{\tilde{q}} = m_{\tilde{g}}$	1.8	2.0	2.3
$m_{\tilde{q}} = 2m_{\tilde{g}}$	1.0	1.3	1.6

GeV¹².

5. Sparticles at the LHC

Sparticle production cross section at the LHC ($\sqrt{s} = 14$ TeV) are dominated by $\tilde{g}\tilde{g}$, $\tilde{g}\tilde{q}$ and $\tilde{q}\tilde{q}$ production. Production of \tilde{g} and \tilde{q} is followed by decays through the usual cascades. The multi-jets + \cancel{E}_T channel has been examined in detail in the literature. (For more detailed discussion, see the talk by C. H. Chen, these proceedings.) In particular, the Atlas collaboration finds the reach capability for $m_{\tilde{g}}$ listed in Table 2¹³.

These numbers have been confirmed by calculations in Ref. 14, where the mass reach is also plotted in the m_0 vs. $m_{1/2}$ plane. Furthermore, it seems a rough measure of $m_{\tilde{g}}$ can be made to 15 – 25%, by reconstructing hemispheric masses. Detailed calculations for other multi-lepton cascade decay topologies are in progress.

What about other sparticles? It has been shown in Ref. 12 that LHC has a reach in $m_{\tilde{\ell}} \sim 250$ GeV by looking for dilepton + \cancel{E}_T events. Furthermore, LHC can see only slightly better than TeV^* in the $\tilde{W}_1\tilde{Z}_2 \rightarrow 3\ell + \cancel{E}_T$ channel (in particular, the “hole” for $\mu > 0$ still persists at LHC). This is because the $\tilde{Z}_2 \rightarrow \tilde{Z}_1 H_\ell$ spoiler mode closes off a higher mass reach. If such a signal is detected, then detailed information on $m_{\tilde{Z}_2} - m_{\tilde{Z}_1}$ can be obtained.

6. Conclusions

In conclusion, only recently has the capability emerged to perform realistic simulations of supersymmetry at hadron or e^+e^- colliders. We see that LEP II and Tevatron both will be able to explore significant regions of parameter space for minimal SUGRA, and if they are lucky, may discover it. However, of the approved facilities, only LHC can perform a definitive search for sparticles below the TeV scale. The capability of ultra-high energy linear e^+e^- colliders was not discussed here, but, depending on energy, may have comparable reach to LHC, and in addition, be able to

extract detailed and precise information on sparticle masses and couplings¹⁵.

7. Acknowledgements

I thank Chih Hao Chen, Jack Gunion, Chung Kao, Ray Munroe, Frank Paige, Heath Pois, John Sender and Xerxes Tata for collaborations on these various projects. In addition, I thank Jack Gunion and all the UC-Davis workers for organizing a swell conference, and for collaborations.

8. References

1. For an historical overview, see S. Dimopoulos, CERN-TH.7531/94 (1994).
2. For phenomenological reviews of SUSY, see H. P. Nilles, Phys. Rep. **110**, 1 (1984); H. Haber and G. Kane, Phys. Rep. **117**, 75 (1985); X. Tata, in *The Standard Model and Beyond*, p. 304, edited by J. E. Kim, World Scientific (1991); R. Arnowitt and P. Nath, *Lectures presented at the VII J. A. Swieca Summer School, Campos do Jordao, Brazil, 1993* CTP-TAMU-52/93; *Properties of SUSY Particles*, L. Cifarelli and V. Khoze, Editors, World Scientific (1993).
3. U. Amaldi, W. de Boer and H. Fürstenau, Phys. Lett. **B260**, 447 (1991); J. Ellis, S. Kelley and D. Nanopoulos, Phys. Lett. **B260**, 131 (1991); P. Langacker and M. Luo, Phys. Rev. **D44**, 817 (1991).
4. F. Paige and S. Protopopescu, in *Supercollider Physics*, p. 41, ed. D. Soper (World Scientific, 1986); H. Baer, F. Paige, S. Protopopescu and X. Tata, in *Proceedings of the Workshop on Physics at Current Accelerators and Supercolliders*, ed. J. Hewett, A. White and D. Zeppenfeld, (Argonne National Laboratory, 1993).
5. D. Decamp *et.al.* (ALEPH Collaboration), Phys. Lett. **B236**, 86 (1990); P. Abreu *et.al.* (DELPHI Collaboration), Phys. Lett. **B247**, 157 (1990); O. Adriani *et.al.* (L3 Collaboration), CERN-PPE-93-31 (1993); M. Akrawy *et.al.* (OPAL Collaboration), Phys. Lett **B240**, 261 (1990); for a review, see G. Giacomelli and P. Giacomelli, CERN-PPE/93-107 (1993).
6. L. Montanet *et. al.* (Review of Particle Properties), Phys. Rev. **D50**, 1173 (1994).
7. H. Baer, C. H. Chen, R. Munroe, F. Paige and X. Tata, Phys. Rev. **D51**, 1046 (1995).
8. M. Paterno, presented at the SUSY 94 Conference, Ann Arbor, MI and M. Paterno, Stony Brook Ph. D. thesis. See also, F. Abe *et. al.*, Phys. Rev. Lett. **69**, 3439 (1992) for an earlier analysis by the CDF Collaboration.
9. H. Baer, C. Kao and X. Tata, Phys. Rev. **D48**, R2978 (1993) and FSU-HEP-941001 (1994); H. Baer, J. Gunion, C. Kao and H. Pois, UCD-94-19 (1994).

10. H. Baer and X. Tata, Phys. Rev. **D47**, 2739 (1993); H. Baer, C. Kao and X. Tata, Phys. Rev. **D48**, 5175 (1993); H. Baer, C. H. Chen, C. Kao and X. Tata, FSU-HEP-950301 (in preparation); see also T. Kamon, J. Lopez, P. McIntyre and J. White, Phys. Rev. **D50**, 5676 (1994) and references therein, although the branching fractions presented differ from those of Baer *et. al.*.
11. H. Baer, J. Sender and X. Tata, Phys. Rev. **D50**, 4517 (1994).
12. H. Baer, C. H. Chen, F. Paige and X. Tata, Phys. Rev. **D49**, 3283 (1994).
13. ATLAS Collaboration, Technical Proposal, CERN/LHCC/94-3 (1994).
14. H. Baer, C. H. Chen, F. Paige and X. Tata, FSU-HEP-940204 (1994).
15. T. Tsukamoto, K. Fujii, H. Murayama, M. Yamaguchi and Y. Okada, KEK preprint 93-146 (1993).

This figure "fig1-1.png" is available in "png" format from:

<http://arxiv.org/ps/hep-ph/9503301v1>

This figure "fig2-1.png" is available in "png" format from:

<http://arxiv.org/ps/hep-ph/9503301v1>